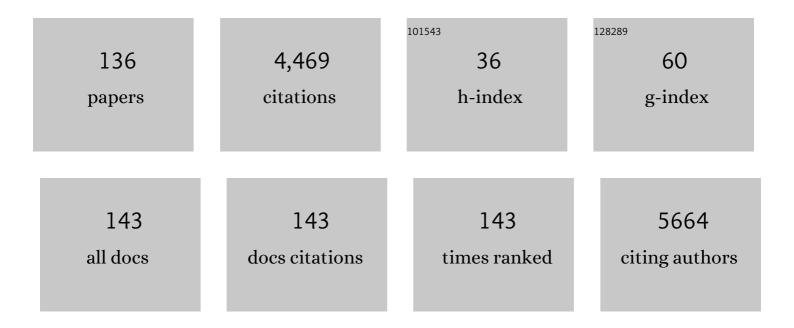
## Gregor Mali

List of Publications by Year in descending order

Source: https://exaly.com/author-pdf/6708052/publications.pdf Version: 2024-02-01



#	Article	IF	CITATIONS
1	Mechanochemically Synthesised Flexible Electrodes Based on Bimetallic Metal–Organic Framework Glasses for the Oxygen Evolution Reaction. Angewandte Chemie - International Edition, 2022, 61, .	13.8	41
2	Metal–biomolecule frameworks (BioMOFs): a novel approach for "green―optoelectronic applications. Chemical Communications, 2022, 58, 677-680.	4.1	7
3	Study of Water Adsorption on EDTA-Modified LTA Zeolites. Nanomaterials, 2022, 12, 1352.	4.1	4
4	Insight into the interdependence of Ni and Al in bifunctional Ni/ZSM-5 catalysts at the nanoscale. Nanoscale Advances, 2022, 4, 2321-2331.	4.6	3
5	Polythiacalixarene-Embedded Gold Nanoparticles for Visible-Light-Driven Photocatalytic CO <sub>2</sub> Reduction. ACS Applied Materials & Interfaces, 2022, 14, 30796-30801.	8.0	8
6	Nanostructured Poly(hydroquinonyl-benzoquinonyl sulfide)/Multiwalled Carbon Nanotube Composite Cathodes: Improved Synthesis and Performance for Rechargeable Li and Mg Organic Batteries. Chemistry of Materials, 2022, 34, 6378-6388.	6.7	3
7	Tailoring microstructural, textural and thermal properties of γ-alumina by modifying aluminum sec-butoxide with ethyl acetoacetate within a sol–gel synthesis. Journal of Physics and Chemistry of Solids, 2021, 148, 109783.	4.0	3
8	Metal-doped carbons from polyurea-crosslinked alginate aerogel beads. Materials Advances, 2021, 2, 2684-2699.	5.4	16
9	Quenchable Porous High-Temperature Polymorph of Sodium Imidazolate, Nalm. Crystal Growth and Design, 2021, 21, 770-778.	3.0	2
10	Hyperfine Coupling Constants in Cu-Based Crystalline Compounds: Solid-State NMR Spectroscopy and First-Principles Calculations with Isolated-Cluster and Extended Periodic-Lattice Models. Journal of Physical Chemistry C, 2021, 125, 4655-4664.	3.1	6
11	Bone diagenesis in the medieval cemetery of Vratislavs' Palace in Prague. Archaeological and Anthropological Sciences, 2021, 13, 1.	1.8	4
12	Technical Note: Post-burial alteration of bones: Quantitative characterization with solid-state 1H MAS NMR. Forensic Science International, 2021, 323, 110783.	2.2	0
13	Scalable Mechanochemical Amorphization of Bimetallic Cuâ <sup>~,</sup> Zn MOF-74 Catalyst for Selective CO <sub>2</sub> Reduction Reaction to Methanol. ACS Applied Materials & Interfaces, 2021, 13, 3070-3077.	8.0	84
14	Liquid-phase sintering of lead halide perovskites and metal-organic framework glasses. Science, 2021, 374, 621-625.	12.6	137
15	Successive Vapor-Phase Guerbet Condensation of Ethanol and 1-Butanol to 2-Ethyl-1-hexanol over Hydroxyapatite Catalysts in a Flow Reactor. ACS Sustainable Chemistry and Engineering, 2021, 9, 17289-17300.	6.7	8
16	The boundary lipid around DMPC-spanning influenza A M2 transmembrane domain channels: Its structure and potential for drug accommodation. Biochimica Et Biophysica Acta - Biomembranes, 2020, 1862, 183156.	2.6	4
17	Effects of a Mixed O/F Ligand in the Tavorite-Type LiVPO <sub>4</sub> O Structure. Chemistry of Materials, 2020, 32, 262-272.	6.7	3
18	Selective defunctionalization of citric acid to tricarballylic acid as a precursor for the production of high-value plasticizers. Green Chemistry, 2020, 22, 7812-7822.	9.0	10

#	Article	IF	CITATIONS
19	Bone diagenesis in the loess deposits of Central Europe: the Celtic site of Radovesice in Bohemia. Archaeological and Anthropological Sciences, 2020, 12, 1.	1.8	4
20	Shape-selective C–H activation of aromatics to biarylic compounds using molecular palladium in zeolites. Nature Catalysis, 2020, 3, 1002-1009.	34.4	41
21	Superoxide formation in Li <sub>2</sub> VO <sub>2</sub> F cathode material – a combined computational and experimental investigation of anionic redox activity. Journal of Materials Chemistry A, 2020, 8, 16551-16559.	10.3	18
22	Innentitelbild: Highly Selective Removal of Perfluorinated Contaminants by Adsorption on All‧ilica Zeolite Beta (Angew. Chem. 33/2020). Angewandte Chemie, 2020, 132, 13770-13770.	2.0	1
23	Design of Effective Catalysts Based on ZnLaZrSi Oxide Systems for Obtaining 1,3-Butadiene from Aqueous Ethanol. ACS Sustainable Chemistry and Engineering, 2020, 8, 16600-16611.	6.7	27
24	Highly Selective Removal of Perfluorinated Contaminants by Adsorption on Allâ€ <b>6</b> ilica Zeolite Beta. Angewandte Chemie - International Edition, 2020, 59, 14086-14090.	13.8	60
25	Highly Selective Removal of Perfluorinated Contaminants by Adsorption on Allâ€ <b>6</b> ilica Zeolite Beta. Angewandte Chemie, 2020, 132, 14190-14194.	2.0	21
26	Ceramic synthesis of disordered lithium rich oxyfluoride materials. Journal of Power Sources, 2020, 467, 228230.	7.8	7
27	Halogenated Metal–Organic Framework Glasses and Liquids. Journal of the American Chemical Society, 2020, 142, 3880-3890.	13.7	83
28	S,O-Functionalized Metal–Organic Frameworks as Heterogeneous Single-Site Catalysts for the Oxidative Alkenylation of Arenes via C–H activation. ACS Catalysis, 2020, 10, 5077-5085.	11.2	45
29	Study of water adsorption on EDTA dealuminated zeolite Y. Microporous and Mesoporous Materials, 2020, 302, 110208.	4.4	13
30	Mechanically Strong Polyurea/Polyurethane-Cross-Linked Alginate Aerogels. ACS Applied Polymer Materials, 2020, 2, 1974-1988.	4.4	32
31	Impact of dehydration and mechanical amorphization on the magnetic properties of Ni( <scp>ii</scp> )-MOF-74. Journal of Materials Chemistry C, 2020, 8, 7132-7142.	5.5	21
32	Unexpected linker-dependent BrÃ,nsted acidity in the (Zr)UiO-66 metal organic framework and application to biomass valorization. Catalysis Science and Technology, 2020, 10, 4002-4009.	4.1	25
33	Polyurea-crosslinked biopolymer aerogel beads. RSC Advances, 2020, 10, 40843-40852.	3.6	25
34	Design of Ti-Beta zeolites with high Ti loading and tuning of their hydrophobic/hydrophilic character. Microporous and Mesoporous Materials, 2019, 288, 109588.	4.4	23
35	Metal-organic framework crystal-glass composites. Nature Communications, 2019, 10, 2580.	12.8	97
36	A Titanium(IV)â€Based Metal–Organic Framework Featuring Defectâ€Rich Tiâ€O Sheets as an Oxidative Desulfurization Catalyst. Angewandte Chemie, 2019, 131, 9258-9263.	2.0	37

#	Article	IF	CITATIONS
37	A Titanium(IV)â€Based Metal–Organic Framework Featuring Defectâ€Rich Tiâ€O Sheets as an Oxidative Desulfurization Catalyst. Angewandte Chemie - International Edition, 2019, 58, 9160-9165.	13.8	99
38	Unraveling the Arrangement of Al and Fe within the Framework Explains the Magnetism of Mixed-Metal MIL-100(Al,Fe). Journal of Physical Chemistry Letters, 2019, 10, 1464-1470.	4.6	26
39	Drug-Membrane Interactions in the Renin Angiotensin System. Series in Bioengineering, 2019, , 339-364.	0.6	1
40	Eumelanin Graphene-Like Integration: The Impact on Physical Properties and Electrical Conductivity. Frontiers in Chemistry, 2019, 7, 121.	3.6	14
41	Layered Zn <sub>2</sub> [Co(CN) <sub>6</sub> ](CH <sub>3</sub> COO) double metal cyanide: a two-dimensional DMC phase with excellent catalytic performance. Chemical Science, 2019, 10, 4868-4875.	7.4	24
42	Active Role of Methanol in Post-Synthetic Linker Exchange in the Metal–Organic Framework UiO-66. Chemistry of Materials, 2019, 31, 1359-1369.	6.7	43
43	Multinuclear Magnetic Resonance Study on Aluminium Sec-butoxide Chelated with Ethyl Acetoacetate in Various Amounts. Croatica Chemica Acta, 2019, 92, 17-28.	0.4	4
44	Catalytic activity of SnO2- and SO4/SnO2-containing clinoptilolite in the esterification of levulinic acid. Microporous and Mesoporous Materials, 2019, 279, 10-18.	4.4	24
45	A metal-organic framework with ultrahigh glass-forming ability. Science Advances, 2018, 4, eaao6827.	10.3	196
46	Structural investigations in pure-silica and Al-ZSM-12 with MTEA or TEA cations. Microporous and Mesoporous Materials, 2018, 263, 236-242.	4.4	3
47	5. Characterization methods. , 2018, , 261-408.		0
48	Metal-organic framework glasses with permanent accessible porosity. Nature Communications, 2018, 9, 5042.	12.8	147
49	Comparative Perturbation Effects Exerted by the Influenza A M2 WT Protein Inhibitors Amantadine and the Spiro[pyrrolidine-2,2′-adamantane] Variant AK13 to Membrane Bilayers Studied Using Biophysical Experiments and Molecular Dynamics Simulations. Journal of Physical Chemistry B, 2018, 122, 9877-9895.	2.6	11
50	High-temperature stabilization of bulk amorphous Al2O3. Journal of Non-Crystalline Solids, 2018, 499, 363-370.	3.1	13
51	Iodide··Â-Ï€ Interactions of Perhalogenated Quinoid Rings in Co-crystals with Organic Bases. Crystal Growth and Design, 2018, 18, 5182-5193.	3.0	19
52	Magnetic resonance spectroscopy approaches for electrochemical research. Physical Sciences Reviews, 2018, 3, .	0.8	1
53	Efficient solid acid catalysts based on sulfated tin oxides for liquid phase esterification of levulinic acid with ethanol. Applied Catalysis A: General, 2018, 560, 119-131.	4.3	37
54	Eu <sup>3+</sup> -Doped Y <sub>3â^'x</sub> Nd <sub>x</sub> Al <sub>3</sub> O <sub>12</sub> garnet: synthesis and structural investigation. Physical Chemistry Chemical Physics, 2017, 19, 3729-3737.	2.8	14

#	Article	IF	CITATIONS
55	Superior Performance of Microporous Aluminophosphate with LTA Topology in Solarâ€Energy Storage and Heat Reallocation. Advanced Energy Materials, 2017, 7, 1601815.	19.5	86
56	Investigation of amorphous and crystalline phosphates in magnesium phosphate ceramics with solid-state 1H and 31P NMR spectroscopy. Ceramics International, 2017, 43, 6571-6579.	4.8	31
57	Exploring the interactions of irbesartan and irbesartan–2-hydroxypropyl-β-cyclodextrin complex with model membranes. Biochimica Et Biophysica Acta - Biomembranes, 2017, 1859, 1089-1098.	2.6	26
58	Growth mechanism and structure of electrochemically synthesized dendritic polymethylsilane molecules. European Polymer Journal, 2017, 90, 162-170.	5.4	5
59	Improved resolution and simplification of the spin-diffusion-based NMR method for the structural analysis of mixed-linker MOFs. Journal of Magnetic Resonance, 2017, 279, 22-28.	2.1	18
60	Synthesis of L-serine modified benzene bridged periodic mesoporous organosilica and its catalytic performance towards aldol condensations. Microporous and Mesoporous Materials, 2017, 251, 1-8.	4.4	14
61	Zr-modified hierarchical mordenite as heterogeneous catalyst for glycerol esterification. Catalysis Communications, 2017, 100, 10-14.	3.3	39
62	<i>Ab initio</i> crystal structure prediction of magnesium (poly)sulfides and calculation of their NMR parameters. Acta Crystallographica Section C, Structural Chemistry, 2017, 73, 229-233.	0.5	13
63	Mechanistic Study of Magnesium–Sulfur Batteries. Chemistry of Materials, 2017, 29, 9555-9564.	6.7	101
64	Tackling the Defect Conundrum in UiO-66: A Mixed-Linker Approach to Engineering Missing Linker Defects. Chemistry of Materials, 2017, 29, 10478-10486.	6.7	102
65	Copolymerization of Norbornene and Norbornadiene Using a cis-Selective Bimetallic W-Based Catalytic System. Polymers, 2017, 9, 141.	4.5	10
66	Poly(hydroquinoyl-benzoquinonyl sulfide) as an active material in Mg and Li organic batteries. Electrochemistry Communications, 2016, 69, 1-5.	4.7	54
67	Post-synthesis bromination of benzene bridged PMO as a way to create a high potential hybrid material. Microporous and Mesoporous Materials, 2016, 236, 244-249.	4.4	9
68	Histidine adsorption on nanostructured cerium oxide. Journal of Electron Spectroscopy and Related Phenomena, 2016, 212, 28-33.	1.7	4
69	Stable Crystalline Forms of Na Polysulfides: Experiment versus Ab Initio Computational Prediction. Chemistry - A European Journal, 2016, 22, 3355-3360.	3.3	13
70	Quinone-formaldehyde polymer as an active material in Li-ion batteries. Journal of Power Sources, 2016, 315, 169-178.	7.8	43
71	Dehydration of AlPO <sub>4</sub> -34 studied by variable-temperature NMR, XRD and first-principles calculations. New Journal of Chemistry, 2016, 40, 4178-4186.	2.8	24
72	A Simple NMRâ€Based Method for Studying the Spatial Distribution of Linkers within Mixedâ€Linker Metal–Organic Frameworks. Angewandte Chemie - International Edition, 2015, 54, 10535-10538.	13.8	55

#	Article	IF	CITATIONS
73	Comparative study of interactions of aliskiren and AT 1 receptor antagonists with lipid bilayers. Biochimica Et Biophysica Acta - Biomembranes, 2015, 1848, 984-994.	2.6	10
74	Structural study of Ni- or Mg-based complexes incorporated within UiO-66-NH2 framework and their impact on hydrogen sorption properties. Journal of Solid State Chemistry, 2015, 225, 209-215.	2.9	19
75	Structural Study of Mg-Based Metal–Organic Frameworks by X-ray Diffraction, 1H, 13C, and 25Mg Solid-State NMR Spectroscopy, and First-Principles Calculations. Journal of Physical Chemistry C, 2015, 119, 7831-7841.	3.1	20
76	Fluorinated Reduced Graphene Oxide as an Interlayer in Li–S Batteries. Chemistry of Materials, 2015, 27, 7070-7081.	6.7	124
77	Xâ€ray Absorption Nearâ€Edge Structure and Nuclear Magnetic Resonance Study of the Lithium–Sulfur Battery and its Components. ChemPhysChem, 2014, 15, 894-904.	2.1	113
78	Preparation, structure and electrochemistry of LiFeBO <sub>3</sub> : a cathode material for Li-ion batteries. Journal of Materials Chemistry A, 2014, 2, 2060-2070.	10.3	58
79	Nitranilic acid hexahydrate, a novel benchmark system of the Zundel cation in an intrinsically asymmetric environment: spectroscopic features and hydrogen bond dynamics characterised by experimental and theoretical methods. Physical Chemistry Chemical Physics, 2014, 16, 998-1007.	2.8	14
80	Indomethacin Embedded into MIL-101 Frameworks: A Solid-State NMR Study. Journal of Physical Chemistry C, 2014, 118, 6140-6150.	3.1	26
81	Distinctive Spectral and Microscopic Features for Characterizing the Three-Dimensional Local Aluminosilicate Structure of Perlites. Journal of Physical Chemistry C, 2014, 118, 26649-26658.	3.1	13
82	Control of the Crystallization Process and Structure Dimensionality of Mg–Benzene–1,3,5-Tricarboxylates by Tuning Solvent Composition. Crystal Growth and Design, 2013, 13, 3825-3834.	3.0	47
83	Interactions of the potent synthetic AT1 antagonist analog BV6 with membrane bilayers and mesoporous silicate matrices. Biochimica Et Biophysica Acta - Biomembranes, 2013, 1828, 1846-1855.	2.6	6
84	Spectroscopic Studies of Structural Dynamics Induced by Heating and Hydration: A Case of Calcium-Terephthalate Metal–Organic Framework. Journal of Physical Chemistry C, 2013, 117, 7552-7564.	3.1	64
85	Study of Hydrothermal Stability and Water Sorption Characteristics of 3-Dimensional Zn-Based Trimesate. Journal of Physical Chemistry C, 2013, 117, 14608-14617.	3.1	20
86	Structural and Dynamical Properties of Indomethacin Molecules Embedded within the Mesopores of SBA-15: A Solid-State NMR View. Journal of Physical Chemistry C, 2012, 116, 2662-2671.	3.1	44
87	Comparative study of the AT1 receptor prodrug antagonist candesartan cilexetil with other sartans on the interactions with membrane bilayers. Biochimica Et Biophysica Acta - Biomembranes, 2012, 1818, 3107-3120.	2.6	19
88	Electrochemically stabilised quinone based electrode composites for Li-ion batteries. Journal of Power Sources, 2012, 199, 308-314.	7.8	67
89	Understanding 6Li MAS NMR spectra of Li2MSiO4 materials (M=Mn, Fe, Zn). Solid State Nuclear Magnetic Resonance, 2012, 42, 33-41.	2.3	20
90	The phase (trans)formation and physical state of a model drug in mesoscopic confinement. Physical Chemistry Chemical Physics, 2011, 13, 16046.	2.8	24

#	Article	IF	CITATIONS
91	A Partial Proton Transfer in Hydrogen Bond O <b>â^'</b> H···O in Crystals of Anhydrous Potassium and Rubidium Complex Chloranilates. Journal of Physical Chemistry A, 2011, 115, 3154-3166.	2.5	23
92	Thermal, dynamic and structural properties of drug AT1 antagonist olmesartan in lipid bilayers. Biochimica Et Biophysica Acta - Biomembranes, 2011, 1808, 2995-3006.	2.6	23
93	Polymorphism in Li2(Fe,Mn)SiO4: A combined diffraction and NMR study. Journal of Materials Chemistry, 2011, 21, 17823.	6.7	55
94	Li <sub>2</sub> FeSiO <sub>4</sub> Polymorphs Probed by <sup>6</sup> Li MAS NMR and <sup>57</sup> Fe Mössbauer Spectroscopy. Chemistry of Materials, 2011, 23, 2735-2744.	6.7	65
95	Spectroscopic Investigation of Ti-Modified Aluminum-Free Zeolite-Beta Crystallization. Chemistry of Materials, 2011, 23, 1337-1346.	6.7	10
96	On the thermal degradation of 3-methylaminopropylamine captured inside the aluminum phosphate analog of ULM-3. Journal of Thermal Analysis and Calorimetry, 2010, 101, 919-924.	3.6	0
97	MnO <sub><i>x</i></sub> Nanoparticles Supported on a New Mesostructured Silicate with Textural Porosity. Chemistry - A European Journal, 2010, 16, 5783-5793.	3.3	40
98	Nitrosobenzene cross-dimerization: Structural selectivity in solution and in solid state. Journal of Molecular Structure, 2010, 979, 22-26.	3.6	13
99	Structure investigation of fluorinated aluminophosphate ULM-3 Al templated by 3-methylaminopropylamine. Journal of Solid State Chemistry, 2010, 183, 1055-1062.	2.9	7
100	Aluminium triplets in dealuminated zeolites detected by 27Al NMR correlation spectroscopy. Microporous and Mesoporous Materials, 2010, 129, 100-105.	4.4	53
101	Thin films of cubic mesoporous aluminophosphates modified by silicon and manganese. Microporous and Mesoporous Materials, 2010, 135, 161-169.	4.4	11
102	6Li MAS NMR spectroscopy and first-principles calculations as a combined tool for the investigation of Li2MnSiO4 polymorphs. Chemical Communications, 2010, 46, 3306.	4.1	68
103	Functionalisation and Structure Characterisation of Porous Silicates and Aluminophosphates. , 2009, , 101-126.		3
104	A spectroscopic study of calcium aluminate gels obtained from aluminium sec-butoxide chelated with ethyl acetoacetate in various ratios. Journal of Sol-Gel Science and Technology, 2009, 50, 58-68.	2.4	18
105	Cross-dimerization of nitrosobenzenes in solution and in solid state. Journal of Molecular Structure, 2009, 918, 19-25.	3.6	25
106	Measuring distances between half-integer quadrupolar nuclei and detecting relative orientations of quadrupolar and dipolar tensors by double-quantum homonuclear dipolar recoupling nuclear magnetic resonance experiments. Journal of Chemical Physics, 2008, 128, 204503.	3.0	29
107	29Si NMR, XRD and HRTEM investigation of Ti-Beta particle formation. Studies in Surface Science and Catalysis, 2008, 174, 817-820.	1.5	0
108	On the Energetic Stability and Electrochemistry of Li <sub>2</sub> MnSiO <sub>4</sub> Polymorphs. Chemistry of Materials, 2008, 20, 5574-5584.	6.7	178

#	Article	IF	CITATIONS
109	Mesoporous Aluminophosphate Thin Films with Cubic Pore Arrangement. Langmuir, 2008, 24, 6220-6225.	3.5	21
110	Solid-State NMR investigation of formation of mesoporous thin films and powders. Studies in Surface Science and Catalysis, 2008, 174, 949-952.	1.5	4
111	Beyond One-Electron Reaction in Li Cathode Materials: Â Designing Li2MnxFe1-xSiO4. Chemistry of Materials, 2007, 19, 3633-3640.	6.7	245
112	Synthesis and structural properties of titanium containing microporous/mesoporous silicate composite (Ti, Al)-Beta/MCM-48. Microporous and Mesoporous Materials, 2007, 99, 3-13.	4.4	24
113	Spin-locking and recoupling of homonuclear dipolar interaction between spin-3/2 nuclei under magic-angle sample spinning. Journal of Magnetic Resonance, 2007, 185, 318-325.	2.1	7
114	Insight into the Short-Range Structure of Amorphous Iron Inositol Hexaphosphate as Provided by31P NMR and Fe X-ray Absorption Spectroscopy. Journal of Physical Chemistry B, 2006, 110, 23060-23067.	2.6	30
115	Positively charged polysilsesquioxane/iodide lonic liquid as a quasi solid-state redox electrolyte for dye-sensitized photo electrochemical cells: Infrared,29SiNMR, and electrical studies. International Journal of Photoenergy, 2006, 2006, 1-8.	2.5	9
116	Manganese-modified hexagonal mesoporous aluminophosphate MnHMA: Synthesis and characterization. Microporous and Mesoporous Materials, 2006, 96, 386-395.	4.4	14
117	Titanium containing microporous/mesoporous composite (Ti,Al)-Beta/MCM-41: Synthesis and characterization. Microporous and Mesoporous Materials, 2006, 95, 76-85.	4.4	23
118	Local environment of iron in the mesoporous hexagonal aluminophosphate catalyst. Microporous and Mesoporous Materials, 2005, 87, 52-58.	4.4	8
119	Anomalous scattering in structural chemistry and biology¶. Crystallography Reviews, 2005, 11, 245-335.	1.5	44
120	Novel Polysilsesquioxaneâ^'l-/l3-Ionic Electrolyte for Dye-Sensitized Photoelectrochemical Cells. Journal of Physical Chemistry B, 2005, 109, 14387-14395.	2.6	50
121	31P NMR as a Tool for Studying Incorporation of Ni, Co, Fe, and Mn into Aluminophosphate Zeotypes. Journal of Physical Chemistry B, 2005, 109, 10711-10716.	2.6	39
122	Double-quantum homonuclear correlation magic angle sample spinning nuclear magnetic resonance spectroscopy of dipolar-coupled quadrupolar nuclei. Journal of Chemical Physics, 2004, 120, 2835-2845.	3.0	90
123	Enhancing sensitivity or resolution of homonuclear correlation experiment for half-integer quadrupolar nuclei. Journal of Magnetic Resonance, 2004, 171, 48-56.	2.1	27
124	Detecting proximities between quadrupolar nuclei by double-quantum NMR. Chemical Communications, 2004, , 868.	4.1	20
125	Solid-State NMR Study of an Open-Framework Aluminophosphate-Oxalate Hybrid. Journal of Physical Chemistry B, 2003, 107, 1286-1292.	2.6	9
126	New Inorganicâ^'Organic Hybrid:  Synthesis and Structural Characterization of an Alumino(oxalato)phosphate. Chemistry of Materials, 2003, 15, 1734-1738.	6.7	14

#	Article	IF	CITATIONS
127	Determination of distances between aluminum and spin-1/2 nuclei using cross polarization with very weak radio-frequency fields. Journal of Chemical Physics, 2002, 117, 3327-3339.	3.0	19
128	Interaction of Dipropylamine Template Molecules with the Framework of as-Synthesized AlPO4-31. Journal of Physical Chemistry B, 2002, 106, 63-69.	2.6	17
129	Framework cobalt and manganese in MeAPO-31 (Me=Co, Mn) molecular sieves. Microporous and Mesoporous Materials, 2002, 55, 203-216.	4.4	31
130	27Al→31P 3QMAS/HETCOR experiment in aluminophosphate molecular sieves. Physical Chemistry Chemical Physics, 2000, 2, 5737-5742.	2.8	11
131	NMR Characterization and Rietveld Refinement of the Structure of Rehydrated AlPO4-34. Journal of Physical Chemistry B, 2000, 104, 5697-5705.	2.6	99
132	spin-lattice relaxation in cobalt-containing aluminophosphate molecular sieves. Solid State Nuclear Magnetic Resonance, 1998, 12, 243-249.	2.3	10
133	Looking into Metal-Organic Frameworks with Solid-State NMR Spectroscopy. , 0, , .		6
134	Study of the iron(III)-modified clinoptilolite in the adsorption of phosphate from aqueous medium: mechanism and kinetics. , 0, 78, 231-240.		6
135	Mechanochemically Synthesised Flexible Electrodes based on Bimetallic Metalâ€organic Framework Glasses for the Oxygen Evolution Reaction. Angewandte Chemie, 0, , .	2.0	7
136	The Unexpected Helical Supramolecular Assembly of a Simple Achiral Acetamide Tecton Generates Selective Water Channels. Chemistry - A European Journal, 0, , .	3.3	0